

INTERPRETATION OF MULTIPLE RESIDUAL GRAVITY ANOMALIES BY SPHERICAL BODIES

S.A. Mehanee*, K.S. Essa and M. Elhussein

Department of Geophysics, Faculty of Science, Cairo University,
Giza, 12613, Egypt. * : salahmehanee@yahoo.com

تفسير الشاذات الثقالية المتبقية للعديد من الأجسام الكروية

الخلاصة: نقدم في هذا البحث طريقة عكسية لتفسير العديد من الشاذات الثقالية المتبقية على طول البروفيل للأجسام الكروية وهذه الطريقة تعتمد على طريقة التدرج المترافق المنظم. تعتمد هذه الطريقة على تحويل متعدد للمعاملات المميزة (الأعماق ومعاملات السعة) للأشكال في المجال اللوغاريتمي لمعاملات النموذج فضلاً عن النطاق الفراغي للمعاملات نفسها. وتطبيق العملية العكسية في النطاق اللوغاريتمي له العديد من الفوائد؛ أولاً يجعل المعاملات اللوغاريتمية وحساسيتها (مصروفة جيكوب) متقاربة ومنتزعة، ثانياً يجعل المعاملات الحساسة متساوية وثالثاً فإنه يفرض الخواص الإيجابية للنموذج التي أساساً تحافظ على التقارب واستقرار الطريقة. وقد تم تطبيق الطريقة على بيانات نظرية ليس بها أخطاء عشوائية، فعينت القيم الحقيقية للأجسام المدفونة وعلاوة على ذلك، وجد أن الطريقة مستقرة وتقوم بحساب المعاملات العكسية للأجسام المدفونة بدقة مقبولة عندما استخدمت بيانات نظرية بها أخطاء عشوائية. تم أيضاً تطبيق الطريقة على مثال حقل من كوبا لاستكشاف الكروم. وبناء على ذلك، فهذه الطريقة نستطيع استخدامها للاستكشاف المعدني وعمل تصوير أرضي ضحل وعميق.

ABSTRACT: The present study developed an inversion scheme for the interpretation of multiple residual gravity anomalies measured along a profile by spherical bodies. It is based on the regularized conjugate gradient method. The scheme simultaneously inverts for the characteristic parameters (depths z 's and the amplitude coefficients A 's) of all approximative bodies in the logarithmic space of model parameters ($\log(z)$ and $\log(|A|)$) rather than in the space of model parameters themselves (z and A). Carrying out the inversion in the logarithmic space of model parameters has a number of important benefits. First, it makes the logarithmic parameters and their corresponding sensitivities (terms of the Jacobian matrix) comparable and balanced. Second, it makes the sensitivity terms dimensionally the same. Third, it imposes the positive property of the model parameters, which essentially maintains the convergence and stability of the scheme. The developed scheme has been successfully verified on synthetic examples without noise; it recovered the true values of all inverse parameters of the underlying bodies. Furthermore, the scheme is stable and can estimate the inverse parameters of the buried target with acceptable accuracy when applied to data contaminated with noise. The validity of the scheme for practical applications has been illustrated on a field example from Cuba for chromite prospecting. The scheme can be applicable for mineral exploration and shallow and deep earth imaging. It can produce non-unique solution and is sensitive to the initial guess choice.

INTRODUCTION

Interpretation of multiple residual gravity anomalies along a profile by several spherical bodies remains of interest in exploration geophysics (e.g., Abdelrahman et al., 1999; Essa, 2007; LaFehr and Nabighian, 2012; Hinze et al., 2013; Long and Kaufmann, 2013). This rationale can be acceptable in cases that the geological settings have isolated bodies. Therefore, fast quantitative interpretation methods based on geometrically simple idealized bodies in the restricted class of spheres can be used to determine the inverse parameters (that is, the depth z , and amplitude coefficient A of each body) of the buried causative bodies from the residual gravity data.

Methods for the interpretation of a single residual gravity anomaly measured along a profile by some geometrically simple body have been developed (see for example Essa, 2014, 2012; Mehanee, 2014; Biswas, 2015; Mehanee and Essa, 2015, and the references therein).

The objective of this paper is to develop a scheme for the interpretation of multiple residual gravity anomalies measured along a profile by geometrically simple bodies in the restricted class of spheres. The scheme inverts the entire observed residual gravity data (rather than just a few characteristic points out of this observed data set) produced by some bodies embedded in the subsurface. Besides, it simultaneously, rather than successively, estimate the inverse parameters (A 's and z 's) of the causative bodies. The algorithm uses the exact forward modeling formula, and employs Tikhonov regularization (Tikhonov and Arsenin, 1977) and the regularized conjugate gradient method in the space of logarithms of the depths and amplitude coefficients ($\log(z)$ and $\log(|A|)$) of each interpretive spherical body) in order to maintain the convergence of the scheme.

This paper is structured as follows. First, we briefly describe the forward modeling problem (direct solution). Second, the formulation of this particular inverse problem, and its solution by the conjugate

gradient method. Third, the accuracy of the developed scheme is verified on numerical models without noise. Fourth, the scheme is applied to noisy data. Finally, we assess and discuss the applicability of the proposed technique to a published field data example from mineral exploration.

Formulation of the forward modeling solution:

The gravity anomaly (g) due to a number (M) of spherical causative bodies (Figure 1) at a point along a profile has a closed-form solution, and is given (Mehanee, 2014) by

$$g(x, z_1, A_1, \dots, z_M, A_M) = \sum_{m=1}^M A_m \frac{z_m}{((x - \Delta x_m)^2 + z_m^2)^{3/2}} \quad (1)$$

where x (m) is the coordinate of the measurement station, z (m) is the depth to the center of the body (the z axis is chosen positive downward), and A (mGal.m^2) is the amplitude coefficient which is given by $\frac{4}{3} \pi \gamma \sigma r^3$ where σ (kg/m^3) is the density contrast, γ ($6.67384 \times 10^{-11} \text{ m}^3 \text{ kg}^{-1} \text{ s}^{-2}$) is the universal gravitational constant, and r (m) is the radius of the body.

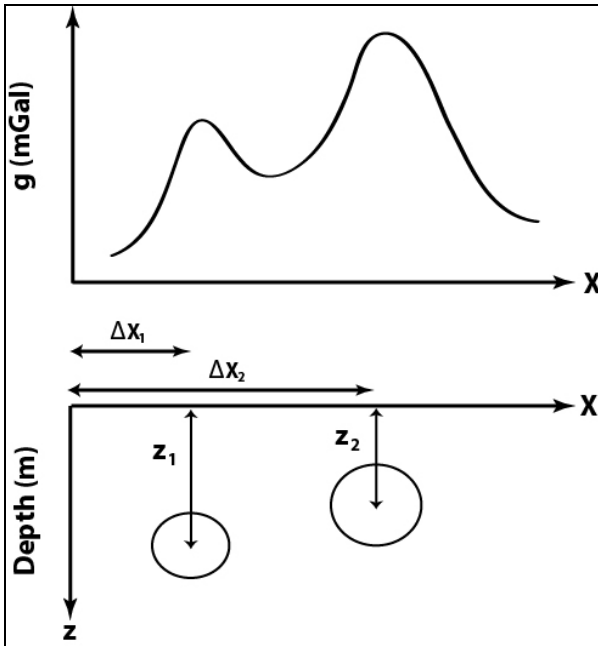


Fig. (1): A sketch showing cross-sectional views, geometries and parameters of two spherical bodies.

1. Formulation of the inverse problem and its proposed solution

In this paper, we seek to solve the discrete nonlinear inverse problem described by the operator equation

$$G(\rho) = g_o, \quad (2)$$

where G is the forward modeling operator acting on ρ to produce some predicted (computed) residual gravity data at a finite number (N) of observation points along a

profile, ρ is the set of model parameters we seek (in our case these are depths z 's and amplitude coefficients A 's), and g_o is a finite set of the measured (observed) residual gravity data obtained along this profile.

The conventional method of solving ill-posed inverse problems is based on the minimization of the Tikhonov parametric functional (Tikhonov et al., 1998; Tarantola, 2005; Mehanee and Essa, 2015):

$$P(\rho) = \phi(\rho) + \alpha S(\rho), \quad (3)$$

where $\phi(\rho)$ is the data misfit functional determined as a square norm of difference between the observed (measured) and predicted (computed) data, $S(\rho)$ is a stabilizing functional, the stabilizer, and α is the regularization parameter (Reginska, 1996).

The parametric (objective) functional subject to minimization is then:

$$P(\rho, g_o) = (G(\rho) - g_o)^T (G(\rho) - g_o) + \alpha \rho^T \rho = \min, \quad (4)$$

where T is the transposition operator. Mehanee (2014) reported that the minimization problem presented in (4) is difficult to solve in the space of the model parameters, as the iterative scheme is unable to converge, when the regularized conjugate gradient method was used. Therefore, the inverse problem (2) is solved in the logarithmic space of the model parameters ($\log(|A_1|), \log(z_1), \dots, \log(|A_M|), \log(z_M)$).

The use of the logarithmic model parameters in inversion has the benefit of making the Frechet (Jacobian) derivatives dimensionally the same, which is a good strategy for balancing the Jacobian terms. Furthermore, the inversion in the logarithmic space of the model parameters forces and guarantees the positivity of the model parameters we seek. Therefore, the new logarithmed space objective functional takes the form:

$$\psi(\bar{\rho}, g_o) = \|\bar{G}(\bar{\rho}) - g_o\|^2 + \alpha \|\bar{\rho}\|^2 = \min \quad (5)$$

where $\bar{\rho} = [\log(z_1) \log(|A_1|) \dots \log(z_M) \log(|A_M|)]^T$ and $\bar{G}(\bar{\rho}) = G(\rho)$. The new nonlinear minimization problem (5) is solved iteratively by the regularized conjugate gradient (CG) method (Zhdanov, 2002; Mehanee, 2014).

2. Numerical models:

We first examine the accuracy of the developed gravity inversion scheme on two noise free examples. After that, the scheme is applied to noisy data.

2.1. Model 1: noise free example:

The gravity response of two spherical bodies ($z_1 = 4$ m, $A_1 = 300$ mGal.m^2 , $z_2 = 4$ m, and $A_2 = 300$ mGal.m^2) is computed at the earth's surface. Using an initial guess of ($z_1 = 1$ m, $A_1 = 20$ mGal.m^2 , $z_2 = 1$ m, and $A_2 = 20$ mGal.m^2) (Table 1), the inversion scheme was applied to this profile. The model parameters recovered from inversion and the true model parameters are tabulated in table 1. This table shows that the

developed scheme has successfully recovered the actual model parameters of the anomalous bodies.

Table (1): Model 1 (noise free data). The initial model parameters used in inversion, the true model parameters, and the model parameters recovered from inversion.

Model parameter	Initial	True	Inversion results
z_1 (m)	1	4	4
A_1 (mGal.m ²)	20	300	300
z_2 (m)	1	4	4
A_2 (mGal.m ²)	20	300	300

Figure 2 shows that the observed data and the predicted response (that is calculated from the solution retrieved from inversion) are coincident with each other.

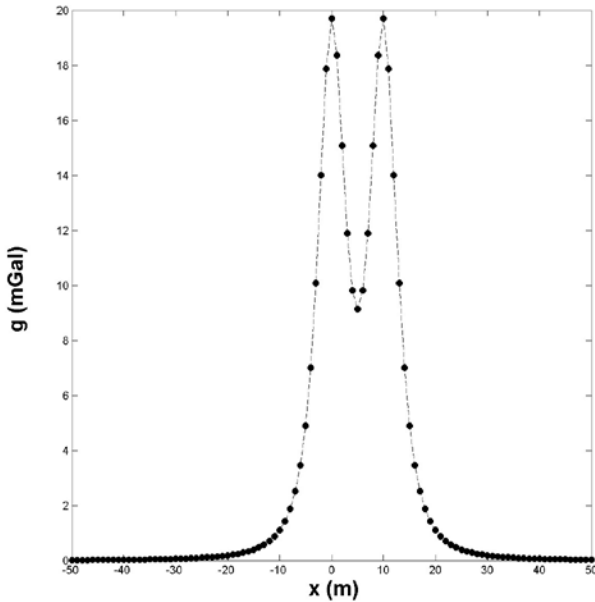


Fig. (2): Model 1 (noise free data): inversion results. The observed and predicated data are coincident with each other. The inversion scheme recovered the actual model parameters (see table 1).

The behavior of the normalized misfit in percentage (defined as $\frac{\|g(\rho) - g_o\|}{\|g_o\|} \times 100\%$) and the objective functional subject to minimization are shown in Figure 3. This figure demonstrates that the inverse scheme is convergent and stable.

In order to get some insights and understand better the reason beyond the good convergence of the log-space algorithm, we have computed the column sensitivities (perturbation of data with respect to model parameters; Fréchet (Jacobian) matrix) from the initial

guesses used in inversion. Figure 4 shows the sensitivities (absolute values) pertinent to the model parameters of the two investigated spheres. This figure shows that the four sensitivity column vectors are comparable in terms of magnitude range which is reflected on the scheme's convergence.

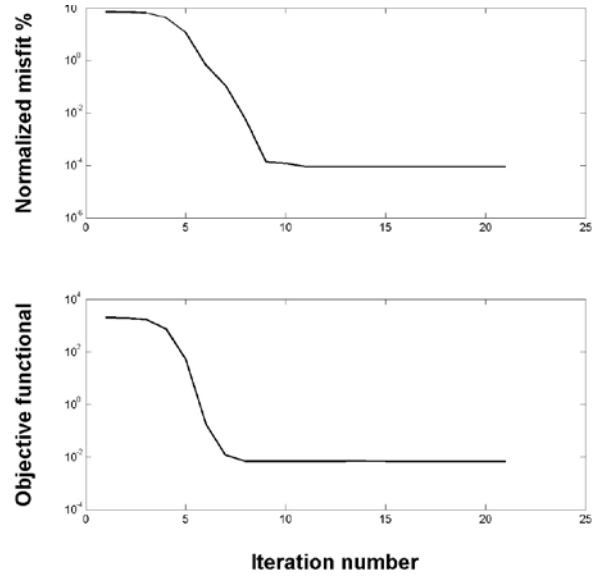


Fig. (3): Model 1 (noise free data): Behavior of the normalized misfit and objective functional subject to minimization.

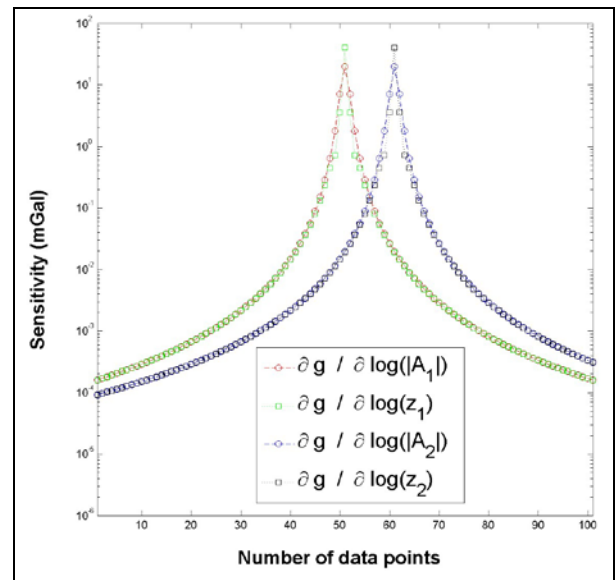


Fig. (4): Model 1 (noise free data): Sensitivity of the model parameters.

2.2. Model 2: noise free example:

The gravity response of two spherical bodies ($z_1 = 10$ m, $A_1 = -50$ mGal.m², $z_2 = 10$ m, and $A_2 = 50$ mGal.m²) is computed at the earth's surface. The inversion scheme was applied to this profile using an initial guess of ($z_1 = 1$ m, $A_1 = -20$ mGal.m², $z_2 = 1$ m,

and $A_2 = 20 \text{ mGal.m}^2$) (Table 2). Table 2 lists the model parameters recovered from inversion and the true model parameters. It is seen from this table that the developed scheme is successful in recovering the actual model parameters of the anomalous bodies.

Table (2): Model 2 (noise free data). The initial model parameters used in inversion, the true model parameters, and the model parameters recovered from inversion.

Model parameter	Initial	True	Inversion results
z_1 (m)	1	10	10
A_1 (mGal.m ²)	-20	-50	-50
z_2 (m)	1	5	5
A_2 (mGal.m ²)	20	50	50

Figure 5 shows that the observed data and the computed response are in good match with each other.

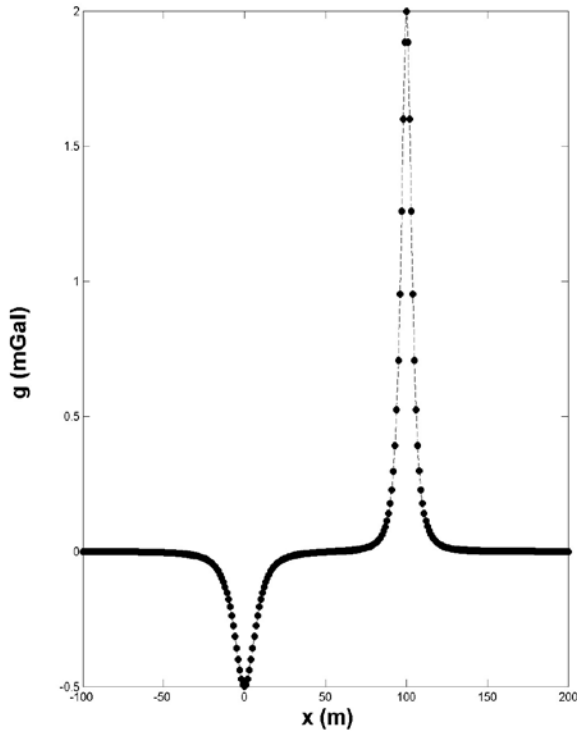


Figure (5): Model 2 (noise free data): inversion results. The observed and predicted data are coincident with each other. The inversion scheme recovered the actual model parameters (see Table 2).

Figure 6 illustrates the progress of the normalized misfit in percentage and the objective functional to be minimized. This figure clearly demonstrates that the inverse scheme is convergent and stable.

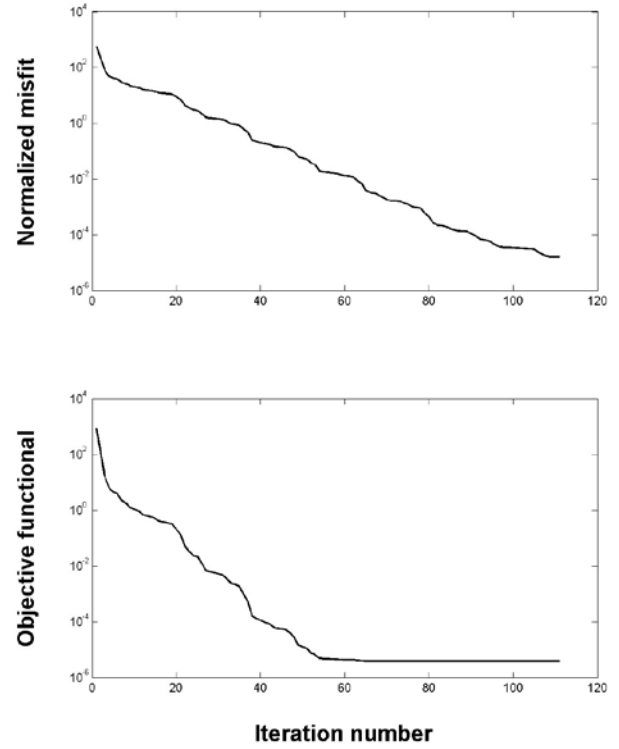


Fig. (6): Model 2 (noise free data): Behavior of the normalized misfit % and objective functional subject to minimization.

Figure 7 shows the sensitivities (absolute values) pertinent to the model parameters of the two investigated spheres. This figure shows that the four sensitivity column vectors are comparable in terms of magnitude range which is reflected on the scheme's convergence.

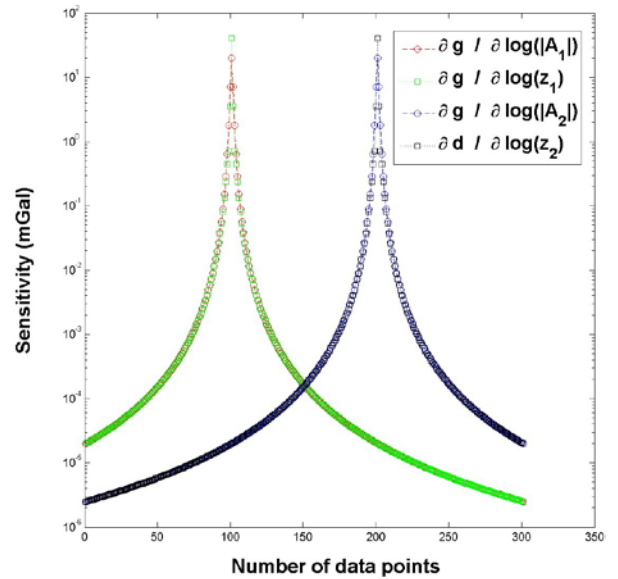


Fig. (7) : Model 2 (noise free data): Sensitivity of the model parameters.

2.3. Model 3: noisy example:

The gravity response of two spherical bodies ($z_1 = 20$ m, $A_1 = -75$ mGal.m², $z_2 = 50$ m, and $A_2 = -400$ mGal.m²) is computed at the earth's surface. This response is then contaminated by 10% noise. The noisy data subject to inversion is shown in Figure 8. Using an initial guess of ($z_1 = 1$ m, $A_1 = -5$ mGal.m², $z_2 = 3$ m, and $A_2 = -1000$ mGal.m²) (Table 3), the inversion scheme was applied to this profile. The iterative process of the scheme terminated when the embedded noise level is reached. The model parameters recovered from inversion ($z_1 = 20$ m, $A_1 = -78$ mGal.m², $z_2 = 3$ m, and $A_2 = 1000$ mGal.m²) and the true model parameters are presented in Table 3. This table shows that the developed scheme has accurately recovered the model parameters of the anomalous bodies.

Table (3): Model 3 (noisy data). The initial model parameters used in inversion, the true model parameters, and the model parameters recovered from inversion.

Model parameter	Initial	True	Inversion results
z_1 (m)	1	20	20
A_1 (mGal.m ²)	-5	-75	-78
z_2 (m)	3	50	53
A_2 (mGal.m ²)	-1000	-400	-448

Figure 8 illustrates that the observed data and the predicted response (that is calculated from the solution generated from inversion) are in good match.

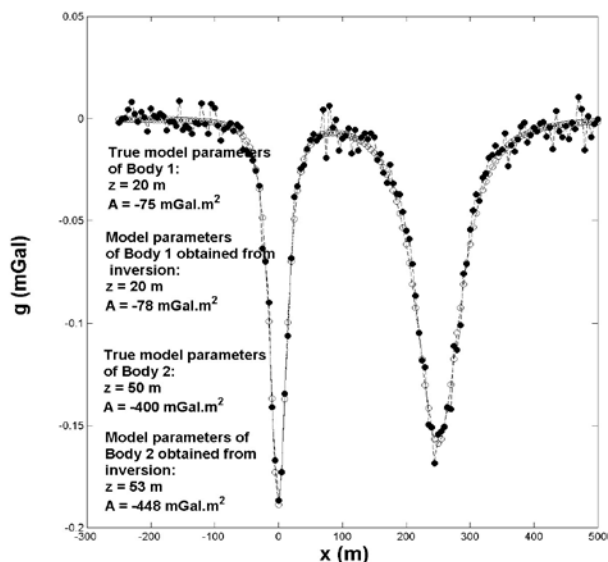


Fig. (8): Model 3 (noisy data): inversion results (see Table 3). The observed and predicated data are shown in solid and open circles.

The behavior of the normalized misfit in percentage and the objective functional subject to minimization are shown in Figure 9. This figure demonstrates that the inverse scheme is convergent and stable.

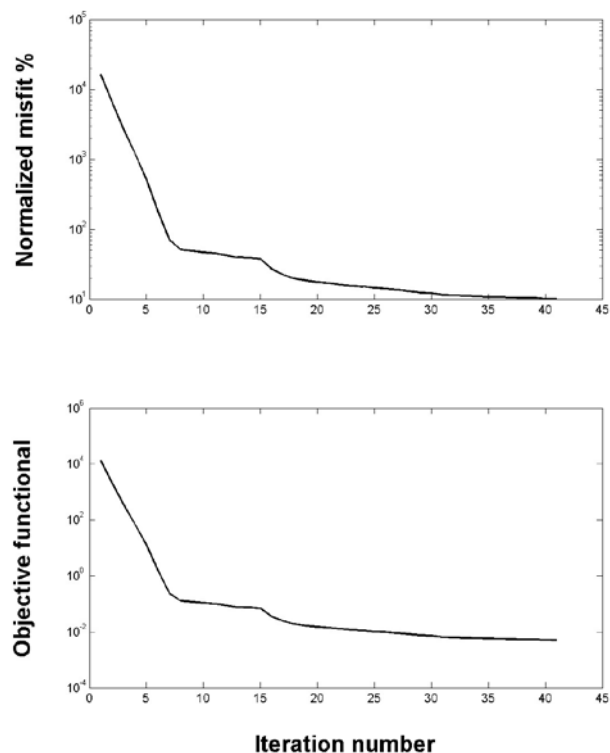


Fig. (9): Model 3 (noisy data): Behavior of the normalized misfit and objective functional subject to minimization.

5. Field data example:

Hammer et al. (1945) measured gravity data in the Camaguey area, Cuba for chromite prospecting. Figure 10 shows the residual gravity anomalies measured over known chromite bodies. Using two different initial guesses, the inversion scheme was applied to this profile. Figures 10 and 11 depict the inversion results and the convergence of the minimization retrieved from Initial guess 1. A normalized misfit of 22.7 % was reached. Using a density contrast of 1500 kg/m³ to the chromite ore (Hammer et al., 1945) and using the depth to the centre (z_1) and the amplitude coefficient (A_1) inferred from inversion, the depth to the top (z_t) and the radius (r) of Body 1, respectively, are 3.24 m and 2.24m. Those of Body 2 are $z_t = 3$ m and $r = 3.9$ m. The corresponding inversion results (obtained at a normalized misfit of 22.7 %) and convergence recovered from Initial guess 2 are illustrated in Figures 12 and 13. Using the aforementioned density contrast, the depth to the top and the radius of Body 1, respectively, are 1.95 m and 1.87 m. Those of Body 2 are $z_t = 2.88$ m and $r = 3.96$ m.

Assuming a density of 4000 kg/m³ to the chromite body (Hammer et al., 1945), the total mass of the two above-mentioned approximative bodies is about 1149 - 1182 tons. Note that prominent part of this total mass is due to Body 2 (that is nearly 1000 tons). The depth to the top, estimated based on uniform spherical body, by Hammer et al. (1945) from this residual gravity profile

for a chromite ore mass of 1000 tons is about 3 m (see Table II of their paper), which is in good agreement with the depth estimated by scheme developed here.

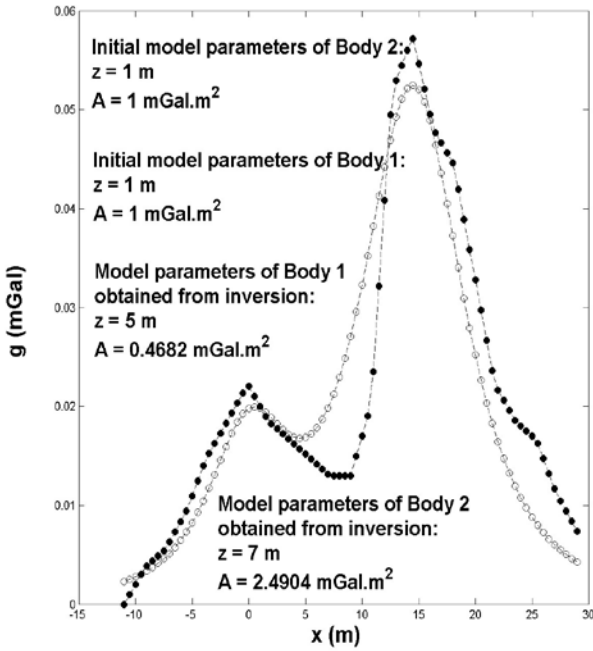


Fig. (10): Field data example: inversion results from initial guess 1. The observed and predicted data are shown in solid and open circles, respectively.

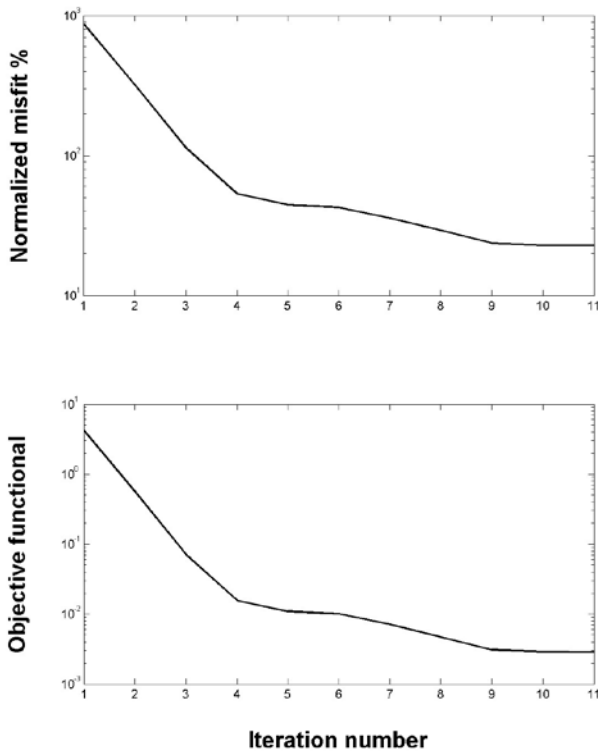


Fig. (11): Field data example: Behavior of the normalized misfit and objective functional subject to minimization obtained from initial guess 1.

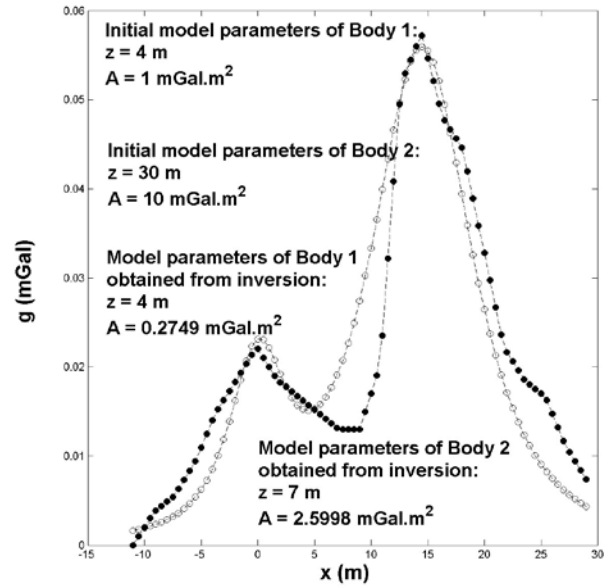


Fig. (12): Field data example: inversion results from initial guess 2. The observed and predicted data are shown in solid and open circles, respectively.

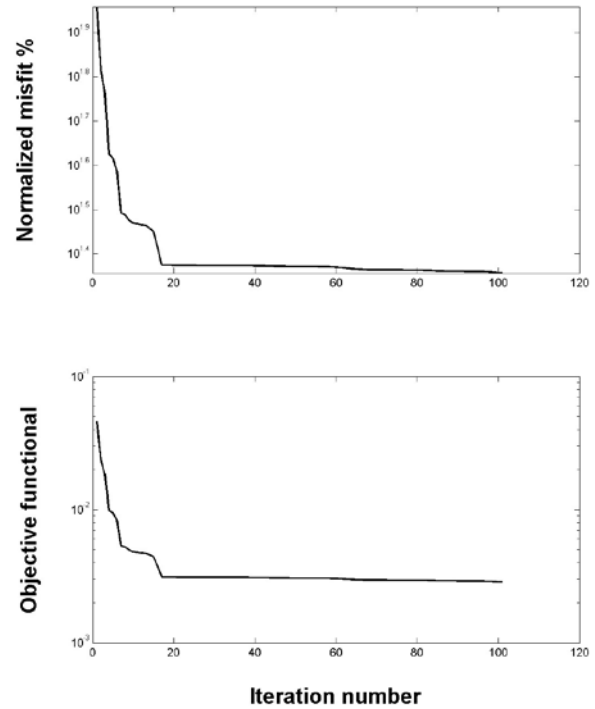


Fig. (13): Field data example: Behavior of the normalized misfit and objective functional subject to minimization generated from Initial guess 2.

SUMMARY AND CONCLUSIONS

We developed a scheme, based on the regularized conjugate gradient method, for the interpretation of multiple residual gravity anomalies measured along a profile by spherical bodies. The scheme simultaneously determines the characteristic parameters (depths z 's, and the amplitude coefficients A 's) of all approximative bodies in the logarithmic space of model parameters

($\log(z)$ and $\log(|A|)$ for each body) rather than in the space of model parameters themselves (z and A for each body).

The developed approach uses the exact closed-form modeling formula, free of any vertical or horizontal numerical derivatives of the measured gravity data, and it simultaneously, rather than successively, recovers the approximative model parameters of the buried anomalous structures. In addition, this approach does not do or involve any averaging for a model parameter(s) during or after the iterative process. Furthermore, the sensitivity (Fréchet) matrix of this approach is evaluated analytically. This technique fits the residual gravity data measured along a profile by some geometrically simple anomalous bodies in the restricted class of spheres..

The developed scheme has been successfully verified on synthetic examples without noise; it recovered the true values of all inverse parameters of the underlying bodies. Furthermore, the scheme is found stable and can estimate the inverse parameters of the buried target with acceptable accuracy when applied to data contaminated with noise.

The validity of this method for practical applications has been illustrated on a field example from Cuba for chromite prospecting. The method can be applicable for mineral exploration, and shallow and deep earth imaging. The obtained inverse parameters should be interpreted in an integrated manner with the known geological and geophysical information. Finally, we note that the method can produce non-unique solution, and is sensitive to the initial guess.

REFERENCES

- Abdelrahman, E.M., Abo-Ezz, E.R. and Radwan, A. H.A., 1999**, A numerical approach to depth determination from residual gravity anomaly due to two structures, *Pure Applied . Geophysics.*, 154, 329-341.
- Biswas, A., 2015**, Interpretation of residual gravity anomaly caused by simple shaped bodies using very fast simulated annealing global optimization, *Geoscience Frontiers*, 1-19.
- Essa, K.S., 2007**, Gravity data interpretation using the s-curves method, *Journal of Geophysics and Engineering*, 4, 2, 204-213.
- Essa, K.S., 2012**, A fast interpretation method for inverse modeling of residual gravity anomalies caused by simple geometry, *Journal of Geological Research*, Volume 2012, Article ID 327037.
- Essa, K.S., 2014**, New fast least-squares algorithm for estimating the best-fitting parameters due to simple geometric-structures from gravity anomalies, *Journal of Advanced Research*,5, 57-65.
- Hammer, S.I., Nettleton, L.L. and Hastings, W.K., 1945**, Gravimeter prospecting for chromite in Cuba, *Geophysics*, 1945, 10, 34-49.
- Hinze, W.J., von Frese, R.R.B. and Saad, A.H., 2013**, Gravity and magnetic exploration: Principles, practices and applications, Cambridge University Press, New York, USA.
- LaFehr, T.R., and Nabighian, M.N., 2012**, Fundamentals of gravity exploration, Society of Exploration Geophysicists, Tulsa, Ok., USA.
- Long, L.T., and Kaufmann, R.D., 2013**, Acquisition and analysis of terrestrial gravity data, Cambridge University Press, New York, USA.
- Mehanee S., 2014**, Accurate and efficient regularized inversion approach for the interpretation of isolated gravity anomalies, *Pure and Applied Geophysics*, 171, 1897-1937.
- Mehanee, S. and Essa, K., 2015**, 2.5D regularized inversion for the interpretation of residual gravity data by a dipping thin sheet: numerical examples and case studies with an insight on sensitivity and non-uniqueness, *Earth, Planets and Space*, 67, 130-158.
- Reginska, T., 1996**, A regularization parameter in discrete ill-posed problems *SIAM J. Sci. Comput.* 3 740-9.
- Tarantola, A., 2005**, Inverse problem theory and methods for model parameters estimation, the Society for Industrial and Applied Mathematics.
- Tikhonov, A.N., and Arsenin, V.Y., 1977**, Solutions of ill-posed problems: John Wiley and Sons.
- Tikhonov, A.N., Leonov, A.S. and Yagola, A.G., 1998**, Nonlinear Ill-Posed Problems Vols 1 and 2, London: Chapman and Hall.
- Zhdanov, M.S., 2002**, Geophysical inversion theory and regularization problems, Elsevier.